creative commons
COMMONS DEED

저작자표시-비영리-변경금지 2.0 대한민국

이용자는 아래의 조건을 따르는 경우에 한하여 자유롭게

- 이 저작물을 복제, 배포, 전송, 전시, 공연 및 방송할 수 있습니다.

다음과 같은 조건을 따라야 합니다:

저작자표시. 귀하는 원저작자를 표시하여야 합니다.

비영리. 귀하는 이 저작물을 영리 목적으로 이용할 수 없습니다.

변경금지. 귀하는 이 저작물을 개작, 변형 또는 가공할 수 없습니다.

- 귀하는, 이 저작물의 재이용이나 배포의 경우, 이 저작물에 적용된 이용허락조건을 명확하게 나타내어야 합니다.
- 저작권자로부터 별도의 허가를 받으면 이러한 조건들은 적용되지 않습니다.

저작권법에 따른 이용자의 권리는 위의 내용에 의하여 영향을 받지 않습니다.

이것은 이용허락규약(Legal Code)을 이해하기 쉽게 요약한 것입니다.

Disclaimer

dCollection

공학석사학위논문

High-precision Submicron Patterning of Organic-Inorganic Hybrid Perovskite Thin Film with Minimizing Edge Effect

가장자리효과를 최소화하는 유-무기 하이브리드 페로브스카이트 박막의 고정밀 서브마이크론 패터닝

2018년 2월

서울대학교 대학원

화학생물공학부

김준수

가장자리효과를 최소화하는 유-무기 하이브리드 페로브스카이트 박막의 고정밀 서브마이크론 패터닝

High-Precision Submicron Patterning of Organic-Inorganic Hybrid Perovskite Thin Film with Minimizing Edge Effect

지도교수 김대형

이 논문을 공학석사 학위논문으로 제출함

2017 년 12 월

서울대학교 대학원

화학생물공학부

김준수

김준수의 석사학위논문을 인준함

2017 년 12 월

위 원 장 선 영은 (인)

부 위 원 장 김 대 형 (인)

위 원 김 태 현 (인)

Abstract

High-precision Submicron Patterning of Organic-Inorganic Hybrid Perovskite Thin Film with Minimizing Edge Effect

Joonsoo Kim

School of Chemical and Biological Engineering

The Graduate School

Seoul National University

Organic-inorganic hybrid perovskite materials have got into the spotlight for their remarkable optoelectronic performance. They are expected to replace the photoactive layer in commercial silicon-based opotoelectronic devices such as solar cell and photodetector. However, their weak stability in various solvents makes them incompatible with conventional photolithography process, which is highly desirable for solution-processed device array.

Although some research groups reported patterning methods to solve this problem, they are suffering from low patterning yield and low patterning quality at the pattern edge. Here, I propose a new patterning method of $CH_3NH_3PbI_3$ by employing SiO_2 trench and dodecyltrichlorosilane, which minimizes shrinkage of $CH_3NH_3PbI_3$ near the pattern edge and makes it possible to realize submicron pattern of $CH_3NH_3PbI_3$ thin film. As a demonstration, Au/$CH_3NH_3PbI_3$/Au photoresistor type photodetector was fabricated by the proposed method. This patterning method provides a new potential for fine-patterned organic-inorganic hybrid material based device.

Keywords: Organic-inorganic hybrid perovskite, patterning, submicron, photodetector, dewetting, trench

Student Number: 2016-21018

Contents

1. Introduction ····· 1

2. Patterning of $CH_3NH_3PbI_3$ thin film ····· 3

2.1. Patterns realized by the proposed method ····· 3

2.2. Characterization of the proposed patterning method 11

3. Photoresistor type photodetector of $CH_3NH_3PbI_3$ patterned by the proposed method ····· 19

3.1. Patterning of single cell photodetectors ····· 19

3.2. Current-voltage (*I-V*) curve of a single cell photodetector depending on light irradiance ····· 21

3.3. *I-V* curve of single cell photodetectors depending on cell size ····· 24

3.4. Photoresponse characterization of a single cell photodetector ····· 28

3.5. Response time characterization of a single cell photodetector ····· 32

4. 24 × 24 array of $CH_3NH_3PbI_3$ photodetectors ····· 35

4.1. Structure of 24 × 24 array of $CH_3NH_3PbI_3$ photodetectors ····· 35

4.2. 24 × 24 $CH_3NH_3PbI_3$ photodetector array demonstration ····· 38

5. Experimental Section ····· 42

5.1. Materials ····· 42

5.2. Preparing $CH_3NH_3PbI_3$ precursor solution ····· 42

5.3. Patterning $CH_3NH_3PbI_3$ with SiO_2 trench and DDTS42

5.4. Patterning $CH_3NH_3PbI_3$ by SoP method ····· 44

5.5. Fabrication of photodetector array ····· 44

5.6. Fabrication of single cell photodetectors ····· 45

5.7. X-ray diffraction characterization ····· 45

5.8. *I-V* characterization of single cell $CH_3NH_3PbI_3$ photodetectors ····· 45

5.9. Pattern size and film thickness characterization ····· 46

5.10. Response time characterization of a single cell photodetector ····· 46

5.11. Absorption spectrum characterization of $CH_3NH_3PbI_3$ ····· 47

5.12. EQE characterization of $CH_3NH_3PbI_3$ photodetector ····· 47

5.13. Multiplexing 24 × 24 $CH_3NH_3PbI_3$ photodetector array ····· 47

5.14. Obtaining images ····· 48

6. Conclusion ····· 49

7. References ····· 50

List of Schemes

1. Procedure of the proposed patterning method.····· 5

2. Schematic description of wetting and dewetting process. ····· 13

3. Structure of the 24 × 24 photodetector array. ····· 36

List of Figures

1. SEM images of circle pattern $CH_3NH_3PbI_3$ film ····· 6

2. SEM image of complex pattern. Brighter area is the perovskite film. ····· 7

3. I (left) and Pb (right) maps of patterned $CH_3NH_3PbI_3$ thin film. ····· 8

4. OM image of unpatterned (top, left) and patterned (top, right) perovskite 2 μm circle pattern array. The bottom images show the circle pattern array at different magnification. ····· 9

5. XRD pattern of patterned (black) and unpatterned (red) $CH_3NH_3PbI_3$ film ····· 10

6. Cross-sectional SEM image of 100 μm circle pattern, by the SoP method (Top) and the proposed method (bottom). ··· 14

7. $CH_3NH_3PbI_3$ film thickness versus the distance from the edge. ····· 15

8. SEM images of 5 μm circle pattern by (a) the SoP method and (b) the proposed method. The region covered by

perovskite are colored in (c) and (d), respectively. ····· 16

9. The plot of areal yield versus pattern size. ····· 17

10. The plot of positional pattern yield versus pattern size of the SoP method and the proposed method. ····· 18

11. Optical image of patterned photoresistor fabricated by (a) the proposed method and (b) the SoP method. ····· 20

12. *I-V* curve of 1.28 × 10^{-2} mm^2 photodetector at different irradiance power using 517 nm laser. ····· 22

13. Plot of current versus irradiance showing linear dynamic range of a 1.28 × 10^{-2} mm^2 photodetector. ····· 23

14. *I-V* curve of single cells with two different size, irradiated by 34.3 mW/cm^2 white light. ····· 25

15. Plot of on and off current versus the size of the photoresistor. The current was measured at 1 V, irradiated by 34.3 mW/cm^2 white light. ····· 26

16. Plot of film thickness versus the diameter of circle-shaped $CH_3NH_3PbI_3$ film. ····· 27

17. Absorption spectrum of $CH_3NH_3PbI_3$ thin film. ····· 29

18. External quantum efficiency (EQE) of 1 mm^2 $CH_3NH_3PbI_3$ photodetector patterned by the proposed method. ····· 30

19. Plot of detectivity versus wavelength of 1 mm^2 $CH_3NH_3PbI_3$ photodetector patterned by the proposed method. ····· 31

20. Setup diagram of response time characterization. ····· 33

21. (a) Temporal response of a 1.28 × 10^{-2} mm^2 photodetector. (b) The 10 % to 90 % risen state and (c) the 90 % to 10 % fallen state. ····· 34

22. Optical image of the fabricated 24 × 24 photodetector array. ····· 37

23. Diagram of the operating photodetector array. ····· 39

24. Images captured by the photodetector array under dark (off) and white light (1.84 mW/cm^2) irradiation (on). ····· 40

25. (a) Scheme of patterned light irradiated on the photodetector array and (b) the obtained image. ····· 41

1. Introduction

Recently, organic-inorganic hybrid perovskite materials have caught great attention due to their high carrier mobility, excellent photo-conversion efficiency (PCE), solution processability, and low-temperature processability.[1-4] They are one of the promising candidate materials to replace commercial silicon for optoelectronic devices in the future.[5] A lot of research has been carried out on their material properties and applications in optoelectronic devices such as solar cells, photodiodes, and LEDs.[5] However, fine patterning of perovskite is limited due to the instability in solvents that are widely used for submicron scale photolithography. In order to overcome this issue, Wang G. *et. al.* proposed selected growth of microplate crystals by using substrate with patterned surface energy, and Feng J. reported a 'liquid knife method' by using guided printing of single crystalline microplates.[6,7] However, in both cases, the shape, size, and position of patterned microplates were not regular nor uniform. Gu L. *et. al.* proposed patterned growth of perovskite nanowires (NWs) based on submicron-resolution template.[8] In this case, however, the process is complicated, and difficulty remains in deposition of electron-transporting layer and hole-transporting layer before and after fabrication of perovskite NWs without damaging them. Wettability assisted patterning (WAP) by Wu J. *et. al.*, and spin-on patterning (SoP) method by Lee W. *et. al.* reported a spin-coating assisted patterning method based on surface energy difference.[9,10] However, their patterned perovskite film shrinks and thins out near pattern edge.

In this work, I propose a new patterning method that realize

$CH_3NH_3PbI_3$ thin film into desired pattern by spin coating, without shrinking and thinning issue. The patterning was achieved by spin-coating of precursor solution on the surface energy and trench-patterned substrate. The precursor solution easily dewets from the dodecyltrichlorosilane (DDTS) layer, however, wets the bottom surface and side wall of SiO_2 trench. The positional and areal yield are near 100 %, which means shrinking hardly occurs. Moreover, the resolution can reach down to submicron range, allowing fine patterns to be realized. For demonstration, a photoresistor type photodetector, which has interdigitated Au electrode under patterned $CH_3NH_3PbI_3$ thin film, was successfully fabricated. Then, isolated photodetectors were integrated into a 24 × 24 array. The photodetector array consists of interdigitated Au electrode, SU8-2 insulator layer, Cu interconnect electrode, SiO_2 and DDTS layer for patterning. The multiplexed photodetector successfully captured an image by a custom-made analyzer.

2. Patterning of $CH_3NH_3PbI_3$ thin film

2.1. Patterns realized by the proposed method

Scheme 1 shows the procedure of the patterning method. First, a clean 2.5 × 2.5 cm^2 bare glass substrate was prepared. Then, SiO_2 layer was deposited using radio-frequency (RF) sputtering. Hydrophobic self-aligned monolayer (SAM), DDTS layer, was deposited onto the SiO_2 layer. Photoresist (S1805) was the spin-coated onto the substrate and patterned by conventional photolithography process. Subsequently, DDTS and SiO_2 layer at the exposed area were removed by reactive ion etching (RIE) to form hydrophilic SiO_2 trench. The substrate was heated at 180 °C for 1 minute, and $CH_3NH_3PbI_3$ precursor solution was spin coated on the heated substrate.[11.] The solution fills the SiO_2 trench, and dewets where DDTS remains on top of SiO_2. **Figure 1** shows scanning electron microscope (SEM) images of patterned $CH_3NH_3PbI_3$ thin film. The diameter of circles are 100 μm, 10 μm, 5 μm, and 800 nm respectively. It shows that all intended positions are patterned without shrinkage. **Figure 2** shows a representative SEM image of patterned $CH_3NH_3PbI_3$ film, showing that complicated patterns can also be achieved. **Figure 3** shows the electron dispersive spectroscopy (EDS) mapping image of 100 μm circle pattern. Pb and I maps coincide with the normal SEM image, implying that $CH_3NH_3PbI_3$ is well patterned. **Figure 4** shows the image of 2 μm circle array pattern covering the entire surface of the glass substrate and its magnified optical microscope (OM) images. $CH_3NH_3PbI_3$ thin film is patterned uniformly throughout the substrate, showing that the proposed patterning method enables uniform wafer scale patterning. **Figure 5** shows the X-ray

diffraction (XRD) peaks of the unpatterned and patterned $CH_3NH_3PbI_3$ film. Representative peaks of $CH_3NH_3PbI_3$ are detected from both cases, confirming successful formation of perovskite. The peaks at 14.1°, 19.9°, 28.4°, 32.9°, and 40.6° represent (110), (112), (220), (310), and (224) planes of tetragonal $CH_3NH_3PbI_3$, respectively.[12.]

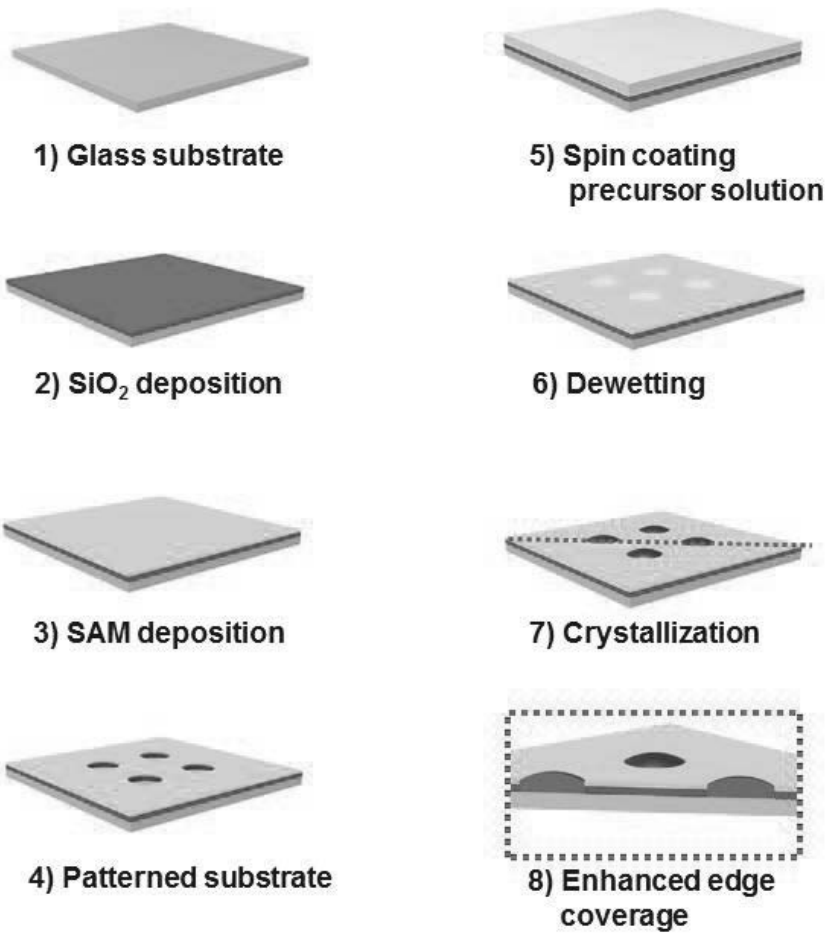

Scheme 1. Procedure of the proposed patterning method.

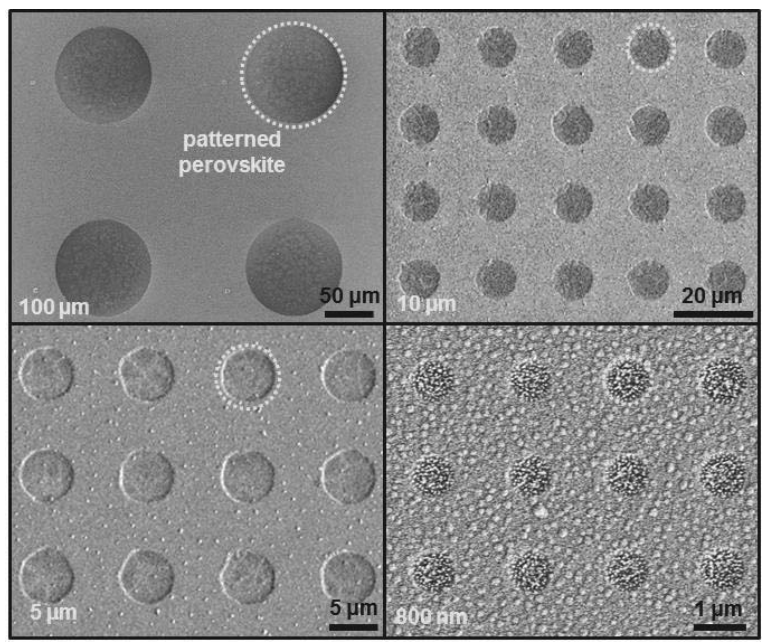

Figure 1. SEM images of circle pattern $CH_3NH_3PbI_3$ film.

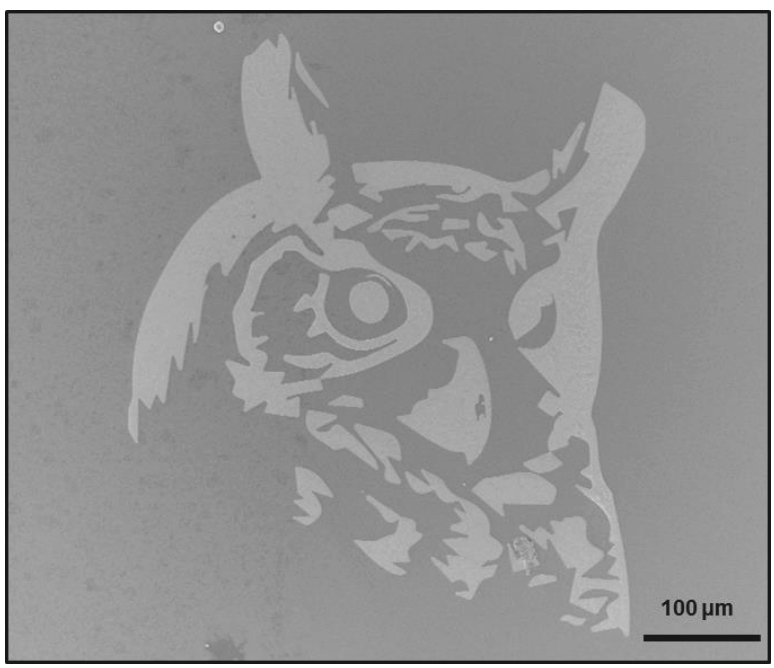

Figure 2. SEM image of complex pattern. Brighter area is the perovskite film.

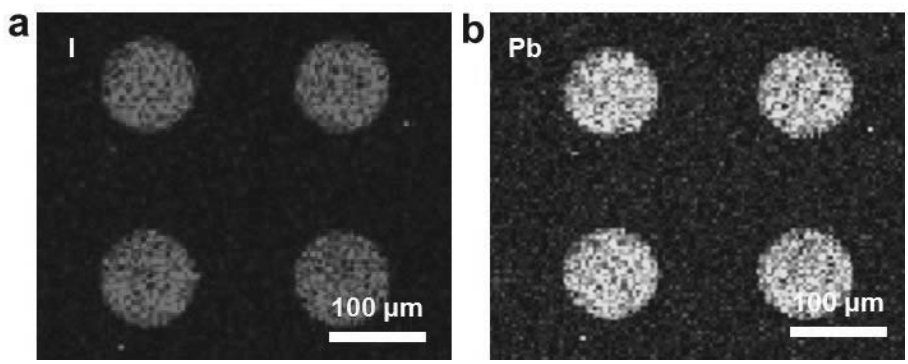

Figure 3. I (left) and Pb (right) maps of patterned $CH_3NH_3PbI_3$ thin film.

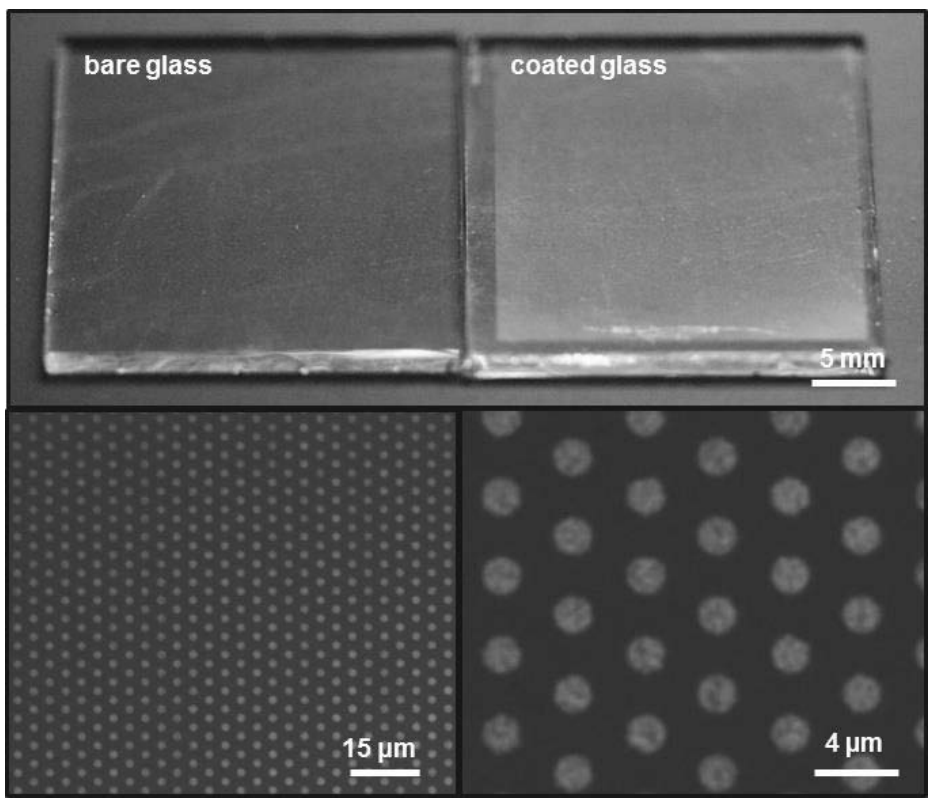

Figure 4. OM image of unpatterned (top, left) and patterned (top, right) perovskite 2 µm circle pattern array. The bottom images show the circle pattern array at different magnification.

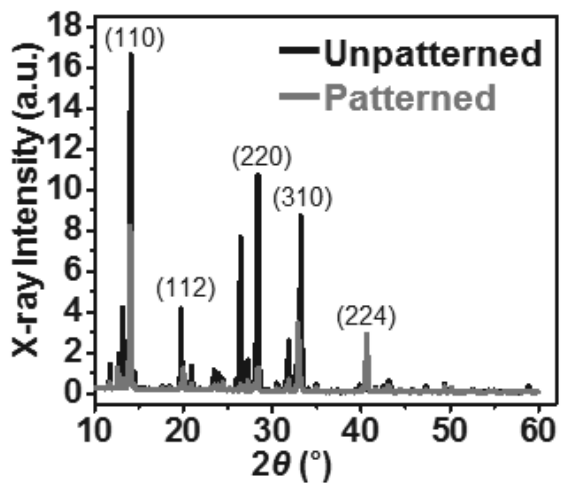

Figure 5. XRD pattern of patterned (black) and unpatterned (red) $CH_3NH_3PbI_3$ film.

2.2. Characterization of the proposed patterning method

During the spin coating step, the precursor solution spreads and covers the whole surface of the substrate. Then, the solution dewets from the location where DDTS is coated on the SiO_2 layer due to weak interaction between DDTS and the solution. However, the solution fills the SiO_2 trench. In this region, the bottom surface and wall become hydrophilic by plasma-activation. Thus, they intimately interact with the precursor solution. The process is shown in **Scheme 2**. Therefore, $CH_3NH_3PbI_3$ can be deposited onto the desired area after crystallization. On the other hand, when it is patterned by the SoP method, which does not include SiO_2 trench layer under SAM layer, the precursor solution at the edge of the desired pattern shrinks to the center and leaves uncovered area. **Figure 6** shows the cross-sectional SEM image of 100 μm circle pattern by the SoP method (top) and the proposed method (bottom). When patterned by the SoP method, about 1 μm from the pattern edge is uncovered, and the thickness of perovskite decreases as it reaches the pattern edge. In the case of the propose method, however, the thickness at the pattern edge is ~200 nm and exhibited no shrinkage at the pattern edge. The $CH_3NH_3PbI_3$ film thickness versus the distance from the edge is shown in **Figure 7**. When the pattern size decreases, the portion of uncovered region becomes larger in the SoP method. **Figure 8** shows the comparison of 5 μm circle pattern formed by the SoP method and the proposed method. No shrinkage is observed when the film is patterned by the proposed method. The pattern area of the film by the SoP method was about 4.2 times smaller than the film patterned by the proposed method. In **Figure 9**, the areal yield of the two methods are compared depending on the size of the pattern. Areal yield decreases as pattern size decreases in the case of the SoP method, while the

areal yield of the proposed method remains almost 100 %. **Figure 10** shows the positional pattern yield of the SoP method and the proposed method. Both methods show higher pattern yield at larger pattern size. The proposed method shows pattern yield about 100 % from 1.5 μm to 100 μm pattern size. In addition, the proposed method constantly shows pattern yield higher than that of the SoP method.

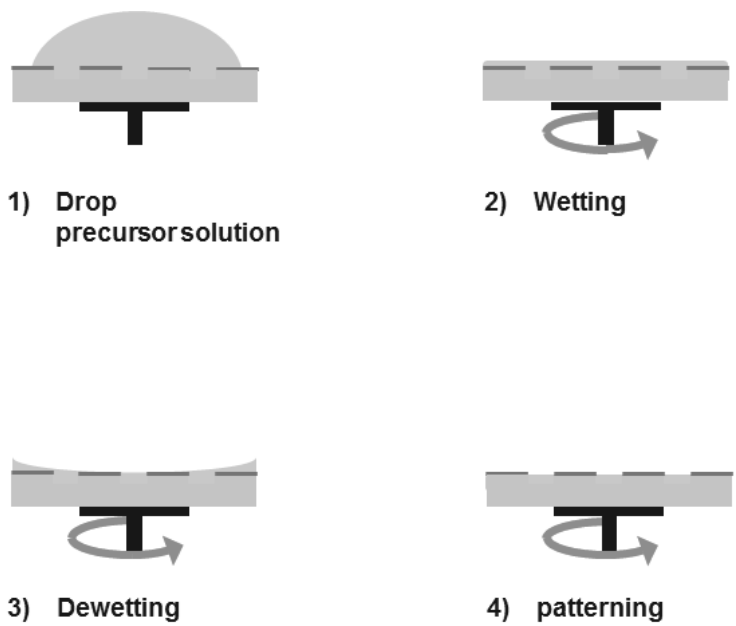

Scheme 2. Schematic description of wetting and dewetting process.

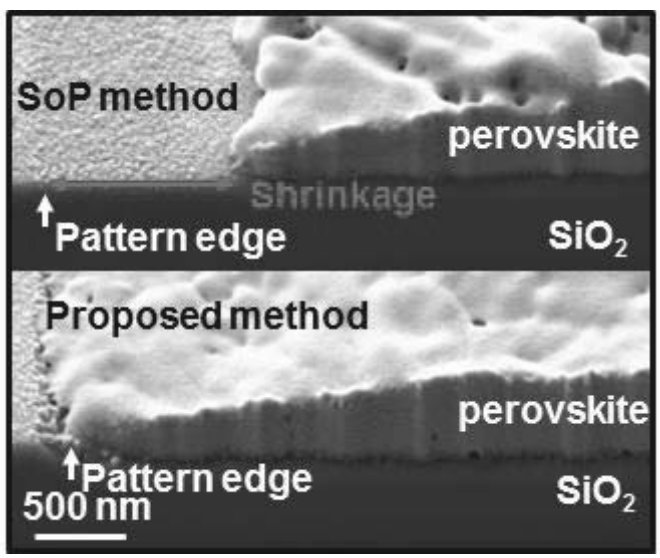

Figure 6. Cross-sectional SEM image of 100 μm circle pattern, by the SoP method (Top) and the proposed method (bottom).

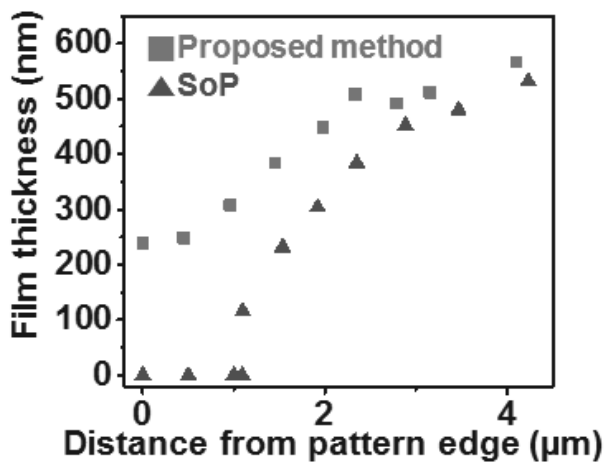

Figure 7. $CH_3NH_3PbI_3$ film thickness versus the distance from the pattern edge.

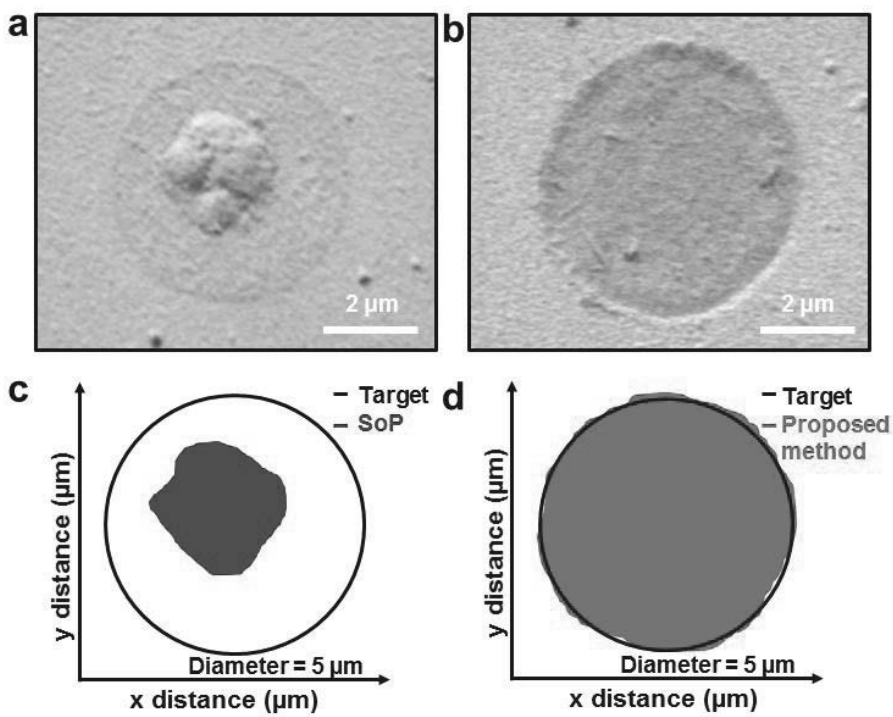

Figure 8. SEM images of 5 μm circle pattern by (a) the SoP method and (b) the proposed method. The region covered by perovskite are colored in (c) and (d), respectively.

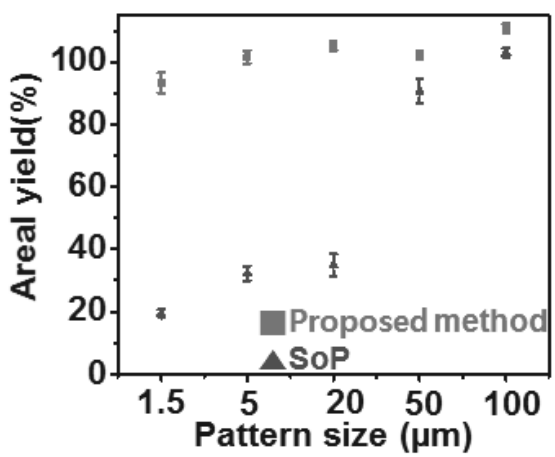

Figure 9. The plot of areal yield versus pattern size.

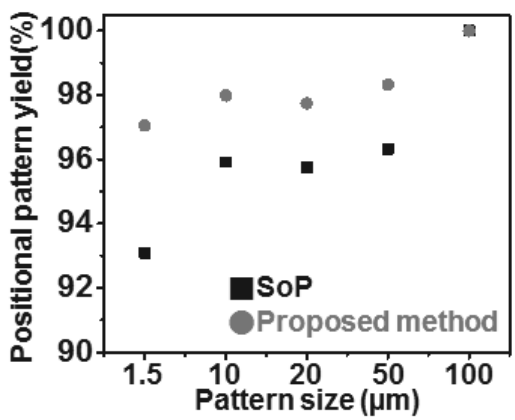

Figure 10. The plot of positional pattern yield versus pattern size of the SoP method and the proposed method.

3. Photoresistor type photodetector of $CH_3NH_3PbI_3$ patterned by the proposed method

3.1. Patterning of single cell photodetectors

The developed patterning method can be used to fabricate the optoelectronic device array. As a stepping stone, we first fabricated patterned $CH_3NH_3PbI_3$ photoresistor using the developed method. As shown in **Figure 11**, the perovskite thin film was deposited between two interdigitated gold electrodes (**Figure 11a**). Compared to the film patterned by the SoP method (**Figure 11b**), the film patterned by the proposed method has more uniform and well-defined shape, which is critical for the performance of photoresistor. The patterning quality of the perovskite film using the SoP method without any rugged sub-layer was high. However, the presence of sub-layer inhibited the uniform formation of patterned thin film. In contrast, the proposed method here enables uniform and high-quality patterning because of the SiO_2 trench, providing a new way of high-quality patterning method regardless of various sub-layers.

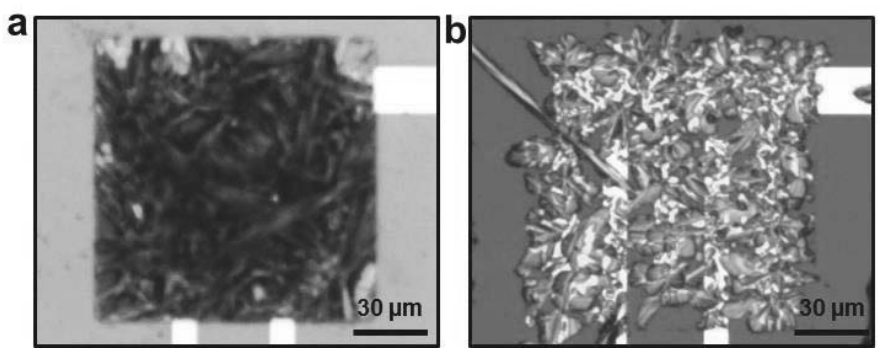

Figure 11. Optical image of patterned photoresistor fabricated by (a) the proposed method and (b) the SoP method.

3.2. Current-voltage (*I-V*) curve of a single cell photodetector depending on light irradiance

When light is irradiated on this photoresistor, electron –hole pairs are generated, and increased number of mobile carrier decreases the resistance of the photodetector. Since the higher light density creates more carriers, the power of the light and the conductance of the photoresistor are in positive relationship. In order to characterize the current level and irradiance characteristics, DC bias from -2 V to 2 V was applied on a 1.28×10^{-2} mm^2 photodetector. At the same time, 517 nm laser with controlled output power was irradiated on the photodetector. The *I-V* curve of the photodetector is shown in **Figure 12**. The slope of the curve increases with increasing output power of the laser. Linear dynamic range of the photodetector was about 70dB at 1 V under 517 nm laser (**Figure 13**), obtained by the following equation where I_{upper} and I_{lower} are the upper and lower edge of LDR, respectively.

$$LDR = 20\log(\frac{I_{upper}}{I_{lower}})$$

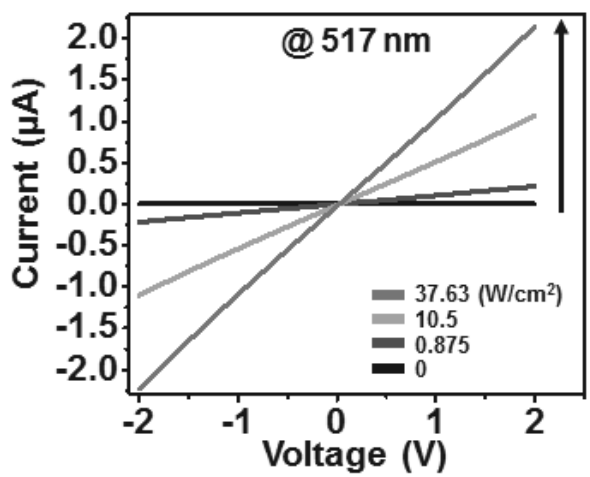

Figure 12. *I-V* curve of 1.28×10^{-2} mm^2 photodetector at different irradiance power using 517 nm laser.

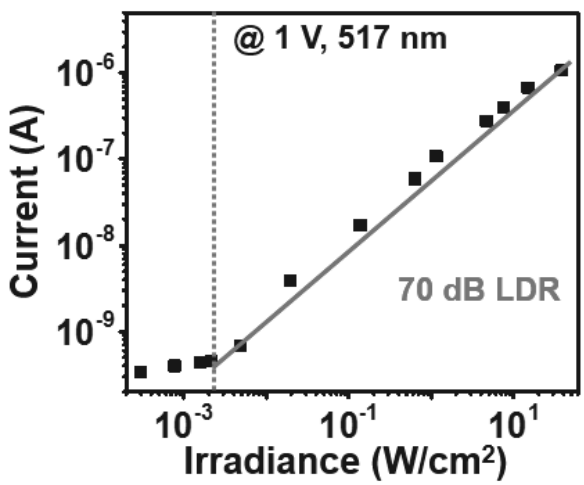

Figure 13. Plot of current versus irradiance showing linear dynamic range of a 1.28×10^{-2} mm^2 photodetector.

3.3. *I-V* curve of single cell photodetectors depending on cell size

Current level of the photodetector under light with constant irradiance power depends on the size of the photodetector. DC voltage from -2 V to 2 V was applied to photodetectors with different cell size and white light with output power of 34.3 mW/cm^2 was irradiated. *I-V* curves of photodetectors with different size are plotted in log scale (**Figure 14**). As the cell size increases, both on and off current increases, maintaining the on-off ratio of ~10^2 (**Figure 15**). The increase of current level by the increase of cell size seems to attribute to two factors. First is the increasing cell area, which makes the single cell photodetector receive more photons. Second is the increasing thickness with increasing area. To confirm this, the thickness of patterned $CH_3NH_3PbI_3$ film realized by the proposed method was characterized by atomic force microscope (AFM) depending on the pattern size. As shown in **Figure 16**, the film thickness increases as the pattern size increases. Therefore, increasing the size of a cell increases the thickness, which makes the cell resistance decrease due to the increase of the cross-section area of a cell.

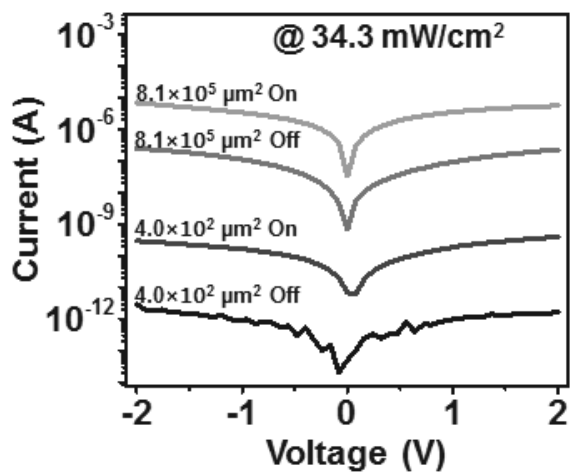

Figure 14. *I-V* curve of single cells with two different size, irradiated by 34.3 mW/cm^2 white light.

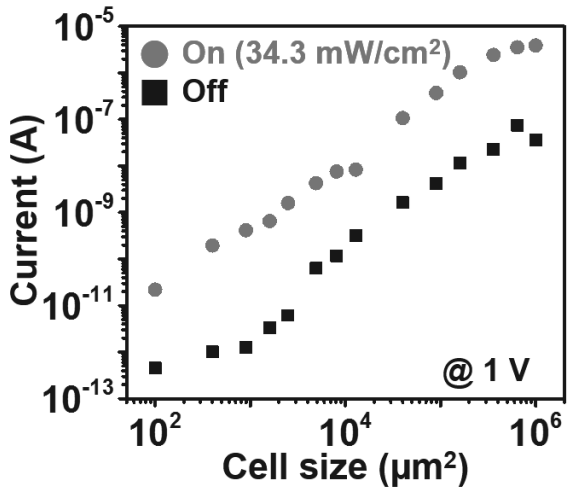

Figure 15. Plot of on and off current versus the size of the photoresistor. The current was measured at 1 V, irradiated by 34.3 mW/cm^2 white light.

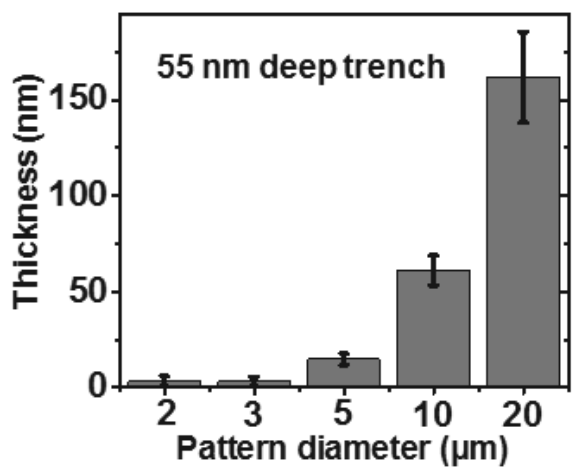

Figure 16. Plot of film thickness versus the diameter of circle-shaped $CH_3NH_3PbI_3$ film.

3.4. Photoresponse characterization of a single cell photodetector

The absorption spectrum of $CH_3NH_3PbI_3$ film coated on glass substrate without patterning was measured by UV-Vis spectrophotometer (**Figure 17**) to elucidate the absorption of patterned perovskite film. The absorption starts near 800 nm and increases as the wavelength gets shorter. The external quantum efficiency (EQE) of a 1 mm^2 $CH_3NH_3PbI_3$ photodetector (**Figure 18**) was measured by solar cell incident photon-to-current efficiency (IPCE) measurement system. Detectivity (**Figure 19**) was also calculated from the EQE by the following equation, where λ is the wavelength, q is the elementary charge, A is the area of the cell, h is the Planck's constant, and c is the speed of light.

$$D^* = \frac{EQE\lambda\sqrt{qA}}{hc\sqrt{2I_{dark}}}$$

Both EQE and detectivity show similar response as the absorption spectrum.

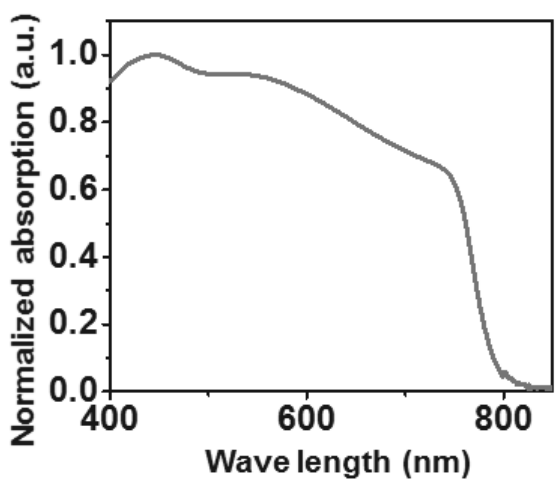

Figure 17. Absorption spectrum of $CH_3NH_3PbI_3$ thin film.

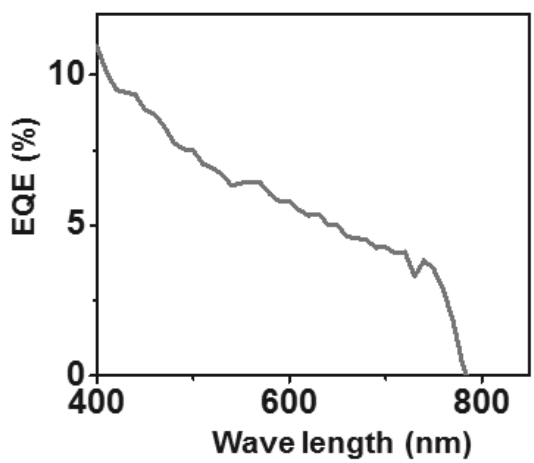

Figure 18. External quantum efficiency (EQE) of 1 mm^2 $CH_3NH_3PbI_3$ photodetector patterned by the proposed method.

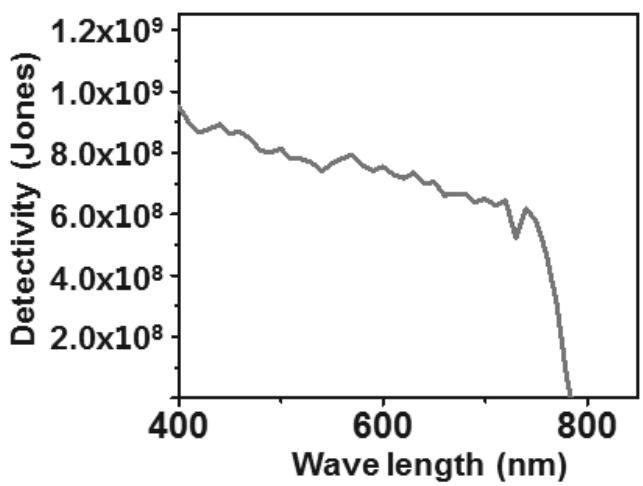

Figure 19. Plot of detectivity versus wavelength of 1 mm^2 $CH_3NH_3PbI_3$ photodetector patterned by the proposed method.

3.5. Response time characterization of a single cell photodetector

Response time is one of the important parameter of the photodetector for its commercialization. The current change induced by the pulsed light of 10 Hz frequency and 507 mW/cm^2 of power irradiated on a 1.28 × 10^{-2} mm^2 photodetector. The photoresistor is connected to a 10 MΩ resistor in series under 20 V DC power as shown in **Figure 20**. The noise was removed from obtained signal by a digital filter and the signal is plotted in **Figure 21**. **Figure 21b** and **Figure 21c** show that the 10% to 90 % rise time and the 90 % to 10% fall time was both about 0.5 ms.

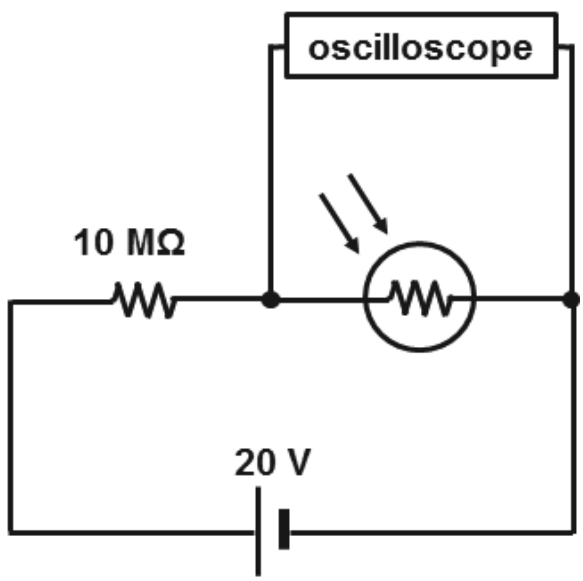

Figure 20. Setup diagram of response time characterization.

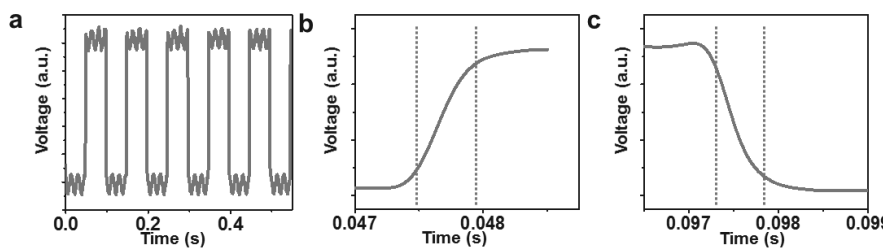

Figure 21. (a) Temporal response of a 1.28×10^{-2} mm^2 photodetector. (b) The 10 % to 90 % risen state and (c) the 90 % to 10 % fallen state.

4. 24 × 24 array of $CH_3NH_3PbI_3$ photodetectors

4.1. Structure of 24 × 24 array of $CH_3NH_3PbI_3$ photodetectors

In order to construct an image sensor array, 576 of 1.28×10^{-2} mm^2 $CH_3NH_3PbI_3$ photodetectors were integrated into a 24 × 24 array. **Scheme 3** shows the structure of the 24 × 24 array. Cr/Au layer was deposited and patterned as array of interdigitated electrodes. SU8-2 insulator layer was deposited where horizontal lines and verticals lines cross over each other. For vertical lines, Cu was deposited and patterned. SiO_2 layer and DDTS layer were deposited sequentially for patterning of $CH_3NH_3PbI_3$. The image of the fabricated array is shown in **Figure 22**.

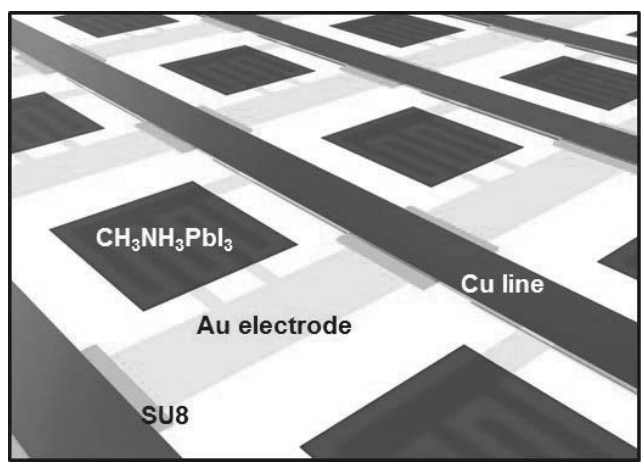

Scheme 3. Structure of the 24 × 24 photodetector array.

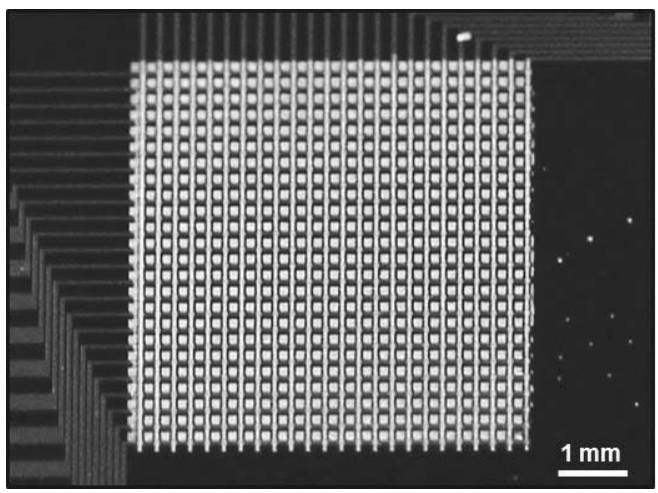

Figure 22. Optical image of the fabricated 24 × 24 photodetector array.

4.2. 24 × 24 $CH_3NH_3PbI_3$ photodetector array demonstration

Fabricated 24 × 24 $CH_3NH_3PbI_3$ photodetector array was connected to a custom-made analyzer for multiplexing for the operation of the 24 × 24 $CH_3NH_3PbI_3$ photodetector array. **Figure 23** shows the diagram of the operating image sensor array. V_{dd} (1 V) is applied to the selected cell. The signals are transmitted to the controller, and converted into an image. **Figure 24** shows images obtained in light off state (left) and light on state (right). 1.84 mW/cm^2 white light was irradiated for the on state. In order to obtain a patterned image, a circle shaped metal mask was covered on the image sensor and 1.84 mW/cm^2 white light was irradiated. The signal was normalized by using the signal obtained from on and off state as the following equation.

$$S = \frac{I - I_{off}}{I_{on} - I_{off}}$$

The image of patterned light being irradiated (**Figure 25a**) and the obtained image (**Figure 25b**) is shown in **Figure 25**. The obtained image shows that the image of the metal mask was detected by the image sensor.

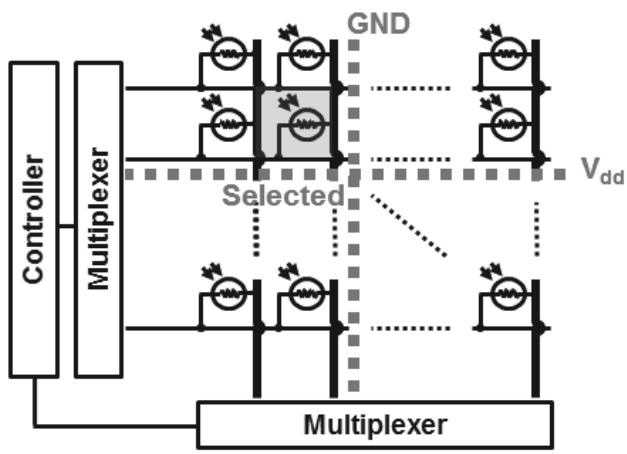

Figure 23. Diagram of the operating photodetector array.

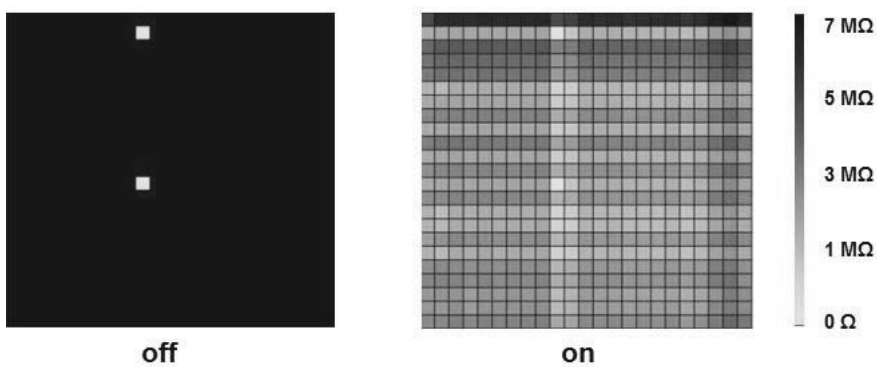

Figure 24. Images captured by the photodetector array under dark (off) and white light (1.84 mW/cm^2) irradiation (on).

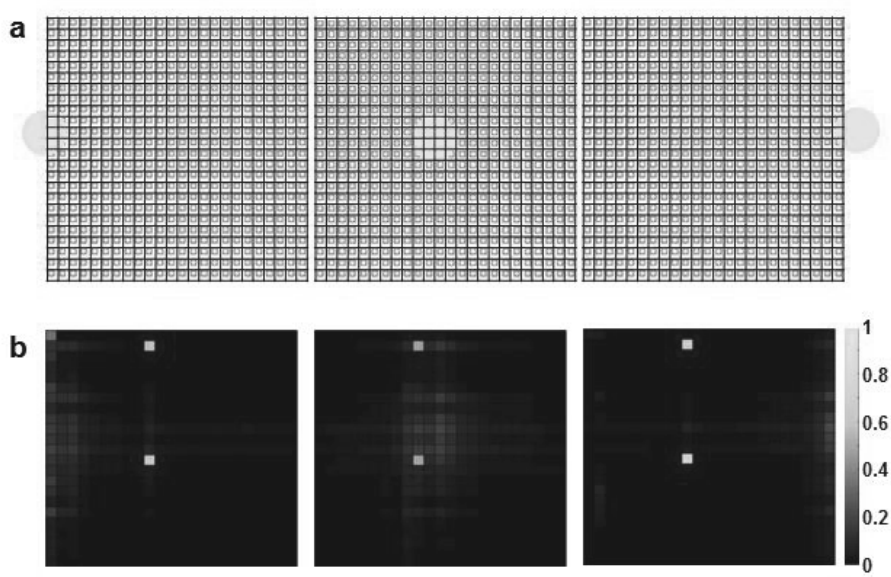

Figure 25. (a) Scheme of patterned light irradiated on the photodetector array and (b) the obtained image.

5. Experimental Section

5.1. Materials

Unless stated, the materials are used as purchased. Dimethyl sulfoxide (anhydrous, ≥99.9%) and dodecyltrichlorosilane (≥99.5% GC) were purchased from Sigma Aldrich (USA). PbI_2 (ultra dry, 99.999%, metal basis) and Cr pieces (99.995%) for thermal evaporation were purchased from Alfa Aesar (USA). CH_3NH_3I was purchased from Dyesol (Austria). γ-butyrolactone (99.5%) was purchased from Junsei (Japan). SiO_2 sputtering target (99.999%) and Cu pellets for thermal evaporation (99.997%) were purchased from Taewon Scientific (Korea). Bare glass substrates were purchased from Wooyang GMS (Korea). Gold pellets for thermal evaporation were purchased from iNexus Inc. (Korea). 8 inch SiO_2 wafers (test grade, P type, (100)) were purchased from LG Siltron (Korea).

5.2. Preparing $CH_3NH_3PbI_3$ precursor solution

Dimethyl sulfoxide (DMSO) and γ-butyrolactone (GBA) were mixed at the molar ratio of 1:2. CH_3NH_3I and PbI_2 were added into the solution at the molar ratio of 1:1 making the concentration of $CH_3NH_3PbI_3$ 0.8M. The mixture was kept at 70 °C and stirred before use.

5.3. Patterning $CH_3NH_3PbI_3$ with SiO_2 trench and DDTS

SAM deposition:

A 25 × 25 × 2 mm^3 bare glass substrate was cleaned with chloroform by sonication for 5 minutes. 0.1 mL of DDTS in was mixed with 200 mL of hexane. For surface modification, the substrate was submerged in the solution for 30 minutes. After 30 minutes, the substrate was taken out and cleaned with ethanol and baked at 120 °C for 30 minutes.

SiO_2 deposition

The substrate was sonicated in chloroform for 5 minutes. Then, the substrate was transferred into the sputter chamber. SiO_2 thin film was deposited by RF sputtering under 20 sccm, 5 mTorr Ar atmosphere at 150W RF power.

Photolithographic patterning:

S1805 photoresist (PR) was spin coated on the substrate at 3000 rpm for 30 seconds and baked at 110 °C for 1 minute. The substrate was exposed to 40 mJ/cm^2 of i-line under a photomask. After development, desired pattern was formed. Then, trenches were created by reactive ion etching (RIE) at O_2 6 sccm, CF_4 60 sccm, 0.055 Torr, 150W RF power. The remaining PR was removed by wiping the substrate with an acetone-soaked swab stick, and cleaning the substrate with isopropyl alcohol (IPA). Then the substrate was transferred to an Argon-filled glove box.

Perovskite coating

The substrate was heated at 180 °C in the glove box prior to the coating. 5 drops of perovskite precursor solution were dropped onto the substrate and the substrate was spin coated at 7000 rpm for 30 seconds.

5.4. Patterning $CH_3NH_3PbI_3$ by SoP method

Patterning perovskite with SoP follows the same procedure of the proposed method except the substrate was etched by RIE at O_2 100 sccm, 0.1 Torr and 50W RF power instead of O_2 6sccm, CF_4 60sccm, 0.055 Torr, 150W RF power, etching DDTS layer but not forming the SiO_2 trench.

5.5 Fabrication of photodetector array

For the substrate of photodetector array, SiO_2 wafer was cut into desired size, which is 2.5 cm × 2.5 cm and ultrasonically cleaned in chloroform. For bottom electrodes, Cr/Au layer, which is 7 nm and 40 nm thick, respectively, was thermally evaporated. The Cr/Au layer was patterned by photolithography with positive PR S1805 and developed with AZ 300 MIF developer. Then, Au layer and Cr layer was etched with Au etchant and Cr etchant, respectively. The remaining PR was removed by rinsing the substrate with acetone. For the insulator layer between horizontal lines and vertical lines, SU8-2 was patterned on locations where vertical lines cross over horizontal lines. In order to pattern Cu top electrodes, negative PR, AZ 2070, was patterned photolithgraphically and developed with AZ 300 MIF. Then, 2 μm thick Cu layer was thermally evaporated on negatively patterned AZ 2070 and lifted off for desired pattern. To pattern $CH_3NH_3PbI_3$ with SiO_2 trench and DDTS, 100 nm thick SiO_2 layer

was deposited by sputtering. On top of the SiO_2 layer, DDTS layer was deposited following the same procedure mentioned before. The DDTS layer was patterned with photolithography using S1805 and etched by RIE at O_2 100sccm, 0.1 Torr, 50W RF power. Subsequently, without opening the chamber, the SiO_2 layer was etched by RIE at O_2 6 sccm, CF_4 60 sccm, 0.055 Torr, 150W RF power. The remaining PR was removed by rinsing the substrate with acetone and rubbing the substrate with a swab stick. Then the substrate was transferred into a glove box. The aforementioned $CH_3NH_3PbI_3$ precursor solution was spin coated on the substrate at 7000 rpm for 30 seconds. The substrate was then annealed at 100 °C for 10 minutes.

5.6. Fabrication of isolated photodetectors

Isolated photodetectors were fabricated exactly the same as photodetector array fabrication procedure, except that the pattern of Cr/Au layer was designed for isolated cells and SU8-2 layer and Cu layer was not deposited.

5.7. X-ray diffraction characterization

X-ray diffraction characteristics of patterned and unpatterned $CH_3NH_3PbI_3$ film was obtained by x-ray diffractometer, D/MAX-2500H (Rigaku, Japan).

5.8. *I-V* characterization of single cell $CH_3NH_3PbI_3$

photodetectors

The *I-V* characterization was conducted by applying DC voltage to a 1.28×10^{-2} mm^2 $CH_3NH_3PbI_3$ photodetector from -2V to 2V. DC voltage was applied and current was read by semiconductor device analyzer, B1500A (Agilent Technologies, USA). B1500A and the photodetector was connected by probe station, MST-5500B (MS Tech, Korea). For light-on state, 34.3 mW/cm^2 white light was irradiated by FOK-100W (Fiber Optic Korea, Korea). For LDR test of $CH_3NH_3PbI_3$ photodetector, 517nm laser beam with varying power was irradiated by LVI-517-500mW (JMJ Korea, Korea).

5.9. Pattern size and film thickness characterization

Circle patterned $CH_3NH_3PbI_3$ film and circle patterned SiO_2 trench without $CH_3NH_3PbI_3$ were prepared. Topography of patterned $CH_3NH_3PbI_3$ film and trench were compared and the thickness of patterned $CH_3NH_3PbI_3$ film was obtained by atomic force microscope, Dimension Icon with ScanAsyst (Bruker, USA).

5.10. Response time characterization of a single cell photodetector

Triple output DC Power supply, U8031A (Keysight, USA), a 10MΩ resistor, and a 1.28×10^{-2} mm^2 $CH_3NH_3PbI_3$ single cell photodetector was connected in series. 20V of DC voltage was applied by U8031A and 10 Hz pulse of 507 mW/cm^2 white light was applied by white LED, U2-HB03 (iMac,

Korea). The voltage applied on the $CH_3NH_3PbI_3$ single cell photodetector was obtained by digital phosphor oscilloscope, DPO 7254C (Tektronix, USA). Digital band-pass filter was used to remove noise.

5.11. Absorption spectrum characterization of $CH_3NH_3PbI_3$

A bare glass substrate was treated by RIE, O_2 100 sccm, 0.1 Torr, 50W. Then, $CH_3NH_3PbI_3$ precursor solution was hot casted on the entire surface. The absorption spectrum of $CH_3NH_3PbI_3$ was characterized by UV-Vis-NIR spectrophotometer, Cary 5000 (Agilent, USA).

5.12. EQE characterization of $CH_3NH_3PbI_3$ photodetector

The EQE of $CH_3NH_3PbI_3$ photodetector was measured by QEX7 (PV Measurements, USA). Incident light with varying wavelength and 1 V of electrical offset voltage was applied to a 1 mm^2 $CH_3NH_3PbI_3$ photodetector.

5.13. Multiplexing 24 × 24 $CH_3NH_3PbI_3$ photodetector array

The fabricated $CH_3NH_3PbI_3$ photodetector array was taken out from the glove box and the remaining $CH_3NH_3PbI_3$ on the contact electrode was removed by 1:2 mixture of DMSO and GBA. The array was connected to source measure units (SMU), NI PXIe-4143 (National Instruments, USA) and

a multiplexer switch module, NI PXI-2530B (National Instruments, USA). 1.84 mW/cm^2 white led patterned by a metal mask was irradiated. The signal was read by a custom-made LabVIEW software (National Instruments, USA).

5.14. Obtaining images

Figure 1 800 nm, **Figure 6**, **Figure 8a**, **Figure 8b** were obtained by SE2 mode of field emission scanning electron microscope (FE-SEM), AURIGA (Carl Zeiss, Germany). **Figure 1** 100 μm and **Figure 2** were obtained by inlens mode of FE-SEM, AURIGA. **Figure 1** 50 μm and 5 μm were obtained by SE2 mode of FE-SEM, MERLIN compact (Carl Zeiss, Germany). **Figure 3** was obtained by EDS mode of FE-SEM, MERLIN compact. Magnified images in **Figure 4**, **Figure 10a**, and **Figure 10b** were obtained by optical microscope (OM), BX41M (Olympus, Japan).

6. Conclusion

In summary, I have proposed a new photolithography-compatible method for patterning organic-inorganic hybrid perovskite thin film by utilizing selective dewetting from SAM layer, and wetting on SiO_2 trench. $CH_3NH_3PbI_3$ thin film patterned by the proposed method showed ~100 % positional and areal pattern yield. Moreover, the pattern resolution reached down to submicron range. This method can be an important method for patterning new photo-absorption layer in commercial image sensor array. As a demonstration, Au/$CH_3NH_3PbI_3$/Au structured photoresistor type photodetector was fabricated using the proposed method. Finally, 24 × 24 array of photodetectors was fabricated. The patterned light was successfully captured by using this image sensor array. Thus, this patterning method enables fabrication of fine devices based on high-performance organic-inorganic hybrid perovskite materials, and has potential for next-generation image sensor fabrication technology.

7. References

1. Wehrenfennig, C.; Eperon, G. E.; Johnston, M. B.; Snaith, H. J; and Herz, L. M., High Charge Carrier Mobilities and Lifetimes in Organolead Trihalide Perovskites. *Adv. Mater.*, **2014**, 26, 1584–1589.

2. Yang, W. S.; Park, B.-W.; Jung, E. H.; Jeon, N. J.; Kim, Y. C.; Lee, D. U.; Shin, S. S.; Seo, J.; Kim, E. K.; Noh, J. H.; Seok, S. I., Iodide management in formamidinium-lead-halide–based perovskite layers for efficient solar cells. *Science*, **2017,** 356, 1376-1379

3. Liu, D.; Kelly, T. L., Perovskite solar cells with a planar heterojunction structure prepared using room-temperature solution processing techniques. *Nat. Photonics*, **2013,** 8, 133.

4. Jung, J. W.; Park, J.-S.; Han, I. K.; Lee, Y.; Park, C.; Kwon, W.; Park, M., Flexible and highly efficient perovskite solar cells with a large active area incorporating cobalt-doped poly(3-hexylthiophene) for enhanced open-circuit voltage. *J. Mater. Chem. A*, **2017,** 5, 12158-12167.

5. Wang, H.; Kim, D. H., Perovskite-based photodetectors: materials and devices. *Chem. Soc. Rev.* , **2017,** 46, 5204-5236.

6. Wang, G.; Li, D.; Cheng, H.-C.; Li, Y.; Chen, C.-Y.; Yin, A.; Zhao, Z.; Lin, Z.; Wu, H.; He, Q.; Ding, M.; Liu, Y.; Huang, Y.; Duan, X., Wafer-scale growth of large arrays of perovskite microplate crystals for functional electronics and optoelectronics. *Sci. Adv.* , **2015,** 1.

7. Feng, J.; Yan, X.; Zhang, Y.; Wang, X.; Wu, Y.; Su, B.; Fu, H.; Jiang, L., “Liquid Knife” to Fabricate Patterning Single-Crystalline Perovskite

Microplates toward High-Performance Laser Arrays. *Adv. Mater.* , **2016,** 28, 3732-3741.

8. Gu, L.; Tavakoli, M. M.; Zhang, D.; Zhang, Q.; Waleed, A.; Xiao, Y.; Tsui, K.-H.; Lin, Y.; Liao, L.; Wang, J.; Fan, Z., 3D Arrays of 1024-Pixel Image Sensors based on Lead Halide Perovskite Nanowires. *Adv. Mater.* , **2016,** 28, 9713-9721.

9. Wu, J.; Chen, J.; Zhang, Y.; Xu, Z.; Zhao, L.; Liu, T.; Luo, D.; Yang, W.; Chen, K.; Hu, Q.; Ye, F.; Wu, P.; Zhu, R.; Gong, Q., Pinhole-Free Hybrid Perovskite Film with Arbitrarily-Shaped Micro-Patterns for Functional Optoelectronic Devices. *Nano Lett.* , **2017,** 17, 3563-3569.

10. Lee, W.; Lee, J.; Yun, H.; Kim, J.; Park, J.; Choi, C.; Kim, D. C.; Seo, H.; Lee, H.; Yu, J. W.; Lee, W. B.; Kim, D.-H., High-Resolution Spin-on-Patterning of Perovskite Thin Films for a Multiplexed Image Sensor Array. *Adv. Mater.* , **2017,** 29.

11. Nie, W.; Tsai, H.; Asadpour, R.; Blancon, J.-C.; Neukirch, A. J.; Gupta, G.; Crochet, J. J.; Chhowalla, M.; Tretiak, S.; Alam, M. A.; Wang, H.-L.; Mohite, A. D., High-efficiency solution-processed perovskite solar cells with millimeter-scale grains. *Science*, **2015,** 347, 522-525.

12. Oku, T., Crystal Structures of $CH_3NH_3PbI_3$ and Related Perovskite Compounds Used for Solar Cells. In *Solar Cells - New Approaches and Reviews*, Kosyachenko, L. A., Ed. InTech: Rijeka, **2015**; p Ch. 03.

요약 (국문 초록)

가장자리효과를 최소화하는 유-무기 하이브리드 페로브스카이트 박막의 고정밀 서브마이크론 패터닝

유-무기 하이브리드 페로브스카이트 물질은 뛰어난 전기광학적 성질로 각광받고 있다. 이들은 태양전지와 광검출기와같은 상용화된 실리콘 기반의 소자에서 광활성층을 대체할 것으로 기대되고 있다. 그러나 다양한 용매에 취약한 특성으로 인해 용액공정으로 소자 어레이를 만드는 데에 있어서 필수적인 전통적인 사진공정이 불가능하였다. 이러한 문제를 해결하기 위한 연구 결과들이 있었으나 패턴의 수율이 낮고 패턴의 질이 떨어지는 문제점이 있었다. 본 논문에서는 SiO_2 박막과 dodecyltrichlorosilane을 활용하여 $CH_3NH_3PbI_3$의 패턴 가장자리에서의 수축을 최소화하고 서브마이크론 범위까지 패턴을 작게 만들 수 있는 패터닝 방법을 제시한다. 이 패터닝 방법을 활용한 소자를 보여주기 위하여 Au/$CH_3NH_3PbI_3$/Au 광저항 방식의 광검출기를 제작하였다. 이 패터닝 방법은 유-무기 하이브리드 물질에 기반한 미세 소자의 제작을 가능하게 한다.

주요어: 유-무기 하이브리드 페로브스카이트, 패터닝, 서브마이크론, 광검출기, 디웨팅, 도랑

학번: 2016-21018